100-Gram Batch Production of Graphene Using High-Power Rapid Joule Heating Method

Authors:

Dan-Na Wu[1†], Jian Sheng[2†], Hai-Gang Lu[1,3*], Si-Dian Li[1*], Yan Li[2*]

Affiliations:

[1]Key Laboratory of Chemical Biology and Molecular Engineering of Ministry of Education, Institute of Molecular Science, Shanxi University, Taiyuan 030006, China.

[2]Beijing National Laboratory for Molecular Sciences, Key Laboratory for the Physics and Chemistry of Nanodevices, College of Chemistry and Molecular Engineering, Peking University, Beijing 100871, China.

[3]Saiyin Materials Co., LTD., JinChuangGu, Taiyuan 030051, China.

[†]These authors contributed equally to this work.

*Corresponding author. Email: luhg@sxu.edu.cn, lisidian@sxu.edu.cn, yanli@pku.edu.cn

Abstract:

Graphene has a vast market demand in the industrial field, but the high cost and complexity of traditional production methods limit its application. The newly developed flash Joule heating method based on capacitor discharge presents a cost-effective production alternative for graphene, but the batch yield is still limited in gram-scale. This study presents a rapid Joule heating (RJH) method based on direct current power discharge to enable large-scale graphene production. Utilizing a high-power RJH system, we can rapidly heat 100 grams of carbon black to 3000°C within minutes, promoting its graphitization transformation, thus achieving a substantial increase in graphene production efficiency. Detailed characterizations confirm the successful synthesis of high-quality turbostratic rapid graphene (RG), with production energy consumption of only ~5 kWh kg^{-1} (0.5 \$ kg^{-1}). Furthermore, by adding boron oxide and melamine as additives, direct mass production of boron,

nitrogen, and nitrogen-boron co-doped RGs can be carried out. Doping modifies the local structure of RG, thereby enhancing its hydrophobicity and electrical conductivity. This work is expected to accelerate the process of low-cost bulk production of graphene and its industrial applications.

Introduction

Graphene, a two-dimensional material with a honeycomb lattice of sp^2-bonded carbon atoms, has garnered significant scientific and industrial attentions due to its exceptional electrical, optical, and mechanical properties.[1-4] Heteroatom doping can further regulate the electronic states and properties of graphene,[5,6] thereby facilitating its applications in various fields. Currently, the annual global production of graphene surpasses 23,000 metric tons. Industries are planning to add graphene in products such as tires, concrete, and asphalt to enhance their properties, which are currently hot areas of commercial investment in graphene.[7] Cost-effective mass production is crucial for achieving the large-scale industrial application of graphene.[8] However, traditional graphene production methods, such as chemical vapor deposition,[9] reduction of graphene oxide,[10] and graphite exfoliation,[11-13] are complex and time-consuming, resulting in high costs.

Since 2020, the flash Joule heating (FJH) method has regarded as an effective approach to convert solid carbon into turbostratic flash graphene in seconds under the combined action of high temperature and electric field.[14-17] In the FJH process, the capacitor tank can discharge instantaneously at approximately 400 V and 1000 A, delivering 400 kW of power to heat a 1.0-gram solid carbon sample to over 3000 °C in milliseconds.[14] By 2023, a small-batch automatic FJH system capable of loading 5.7 grams of metallurgical coke per batch had been designed, with a production capacity of 1.1 kg of graphene in 1.5 hour.[18] Scaling up this automatic FJH system to produce larger batches of graphene requires additional capacitors. For instance, producing 100 g of graphene per batch would necessitate approximately 480 capacitors of 13 mF each, posing significant equipment volume and safety challenges due to the 500-voltage requirement.

Prior to the advent of the FJH method, the rapid Joule heating (RJH) techniques powered by direct current had been rapidly developed and widely applied in various fields, including the graphitization of carbon fibers,[19] the synthesis of high-entropy alloys,[20] and the rapid sintering of ceramics.[21] The RJH process has similar advantages to the FJH process, especially in extremely high energy efficiency and extremely ultrafast heating rate. However, the equipment cost of the RJH process is more economical than that of the FJH process. Compared to the high-power output of 400 kW in the FJH method, previously reported RJH method operates with a power supply of no more than 3 kW in laboratory but can sustain discharges from microseconds to hours. By increasing the power, the RJH method can heat a large batch of samples to a high temperature of 3000°C, which is expected to enable a similar process as FJH in converting solid carbon sources into graphene.

Here, we demonstrate a high-power RJH system that aims to directly convert 100 grams of carbon black into graphene in one batch, making graphene to be produced more efficient, energy-saving, and cost-effective. By adding boron oxide and melamine additives to the carbon black, we can mass produce heteroatom-doped graphene directly and further investigated the effects of these additives on the crystal structure, hydrophobicity, and conductivity of the generated graphene. The RJH system present in this work potentially unlocking new avenues for the large-scale production of graphene.

Results and discussion

RJH process for mass production of graphene

RJH process was conducted using the Saiyin scale-up Joule heating system (Fig. 1a and S1). This system is powered by a 40 kW direct current (DC) power supply, which can deliver output currents ranging from 0 A to 400 A and voltages ranging from 0 V to 100 V. It is also equipped with a Siemens programmable logic controller (PLC), a vacuum box, and an infrared radiation (IR) temperature sensor with a range of 400 °C to 3600 °C. The sample was placed in a vertical quartz tube secured on a sample holder by two graphite electrodes. To ensure the sample powder maintains good

conductivity during heating, the upper electrode is pressed tightly by four springs. Additionally, the sample holder is placed on insulating plates to ensure safety during discharge.

The raw material chosen for graphene production is conductive carbon black, which possesses properties of high carbon content (>98%) and low volatility. Granulated carbon black was utilized to prevent dusting. Under mild vacuum conditions (about –0.098 MPa), carbon black grains were slightly compressed in the quartz tube, resulting in a sample column with an electric resistance of less than 5 ohms. The amount of carbon black per batch, which is 100 g, exceeds the previously reported maximum mass by ~17.5 times (Fig. 1b).[18] Throughout the entire Joule heating process, the temperature signal was monitored in real-time by the temperature sensor, and transmitted to the PLC's PID (Proportional-Integral-Derivative) controller. The controller adjusts the output voltage and current of power supply to manage the heating, maintaining, and cooling phases, ensuring the maximum temperature is controllable at approximately 3000 °C for 5 seconds. The resulting product weighed 96.5 g and exhibited black and gray colors (Fig. 1c), similar to the appearance of flash graphene.[14] Transmission electron microscopy (TEM) images show that the product consists of multi-layer graphene with a size of several tens of nanometers (Fig. 1d-e).

The temperature profile during the Joule heating process, including heating to 3000 °C, maintaining, and cooling to 400 °C, is shown in Fig. 1f. The corresponding voltage, current, and resistance are presented in Fig. S2. By analyzing the trend of temperature curve changes, the RJH process can be divided into pre-heating (<2300 °C) and graphitization (>2300 °C) phases.[22] In the pre-heating stage, the current was less than 50 A due to the high resistance of 100 g of carbon black grains, and the sample took about 243 s to gradually heat up from room temperature to 2300 °C. With the increase in temperature, the sample became less compact due to the release of gas, leading to an increase in resistance. Subsequently, the compressed springs gradually pushed the upper graphite electrode descend to maintain tight contact between the carbon black grains. In the subsequent graphitization process, the sample was rapidly heated to 3000 °C within 1s, accompanied by a peak discharge

current of 320 A. Once the PLC controller's PID program adjusts the discharge current to maintain 3000 °C for 5 s (Fig. 1g), the power was turned off, and the sample began to cool gradually to room temperature. Both heating and cooling rates of Joule heating method significantly higher than those of traditional muffle furnaces, justifying the term of "rapid".

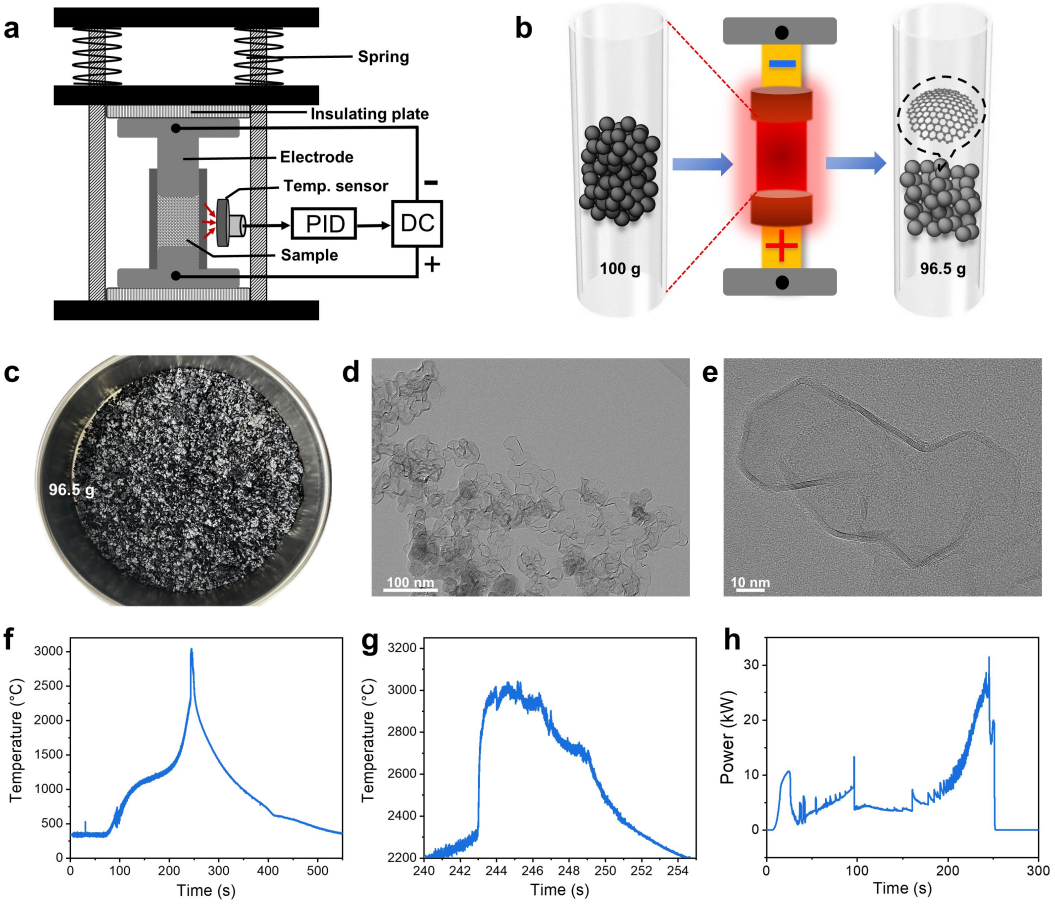

Figure 1. RJH production of graphene. (a) Schematic of high-power RJH equipment. (b) Scale-up of Joule heating processes. (c) Photo of graphene grains prepared from conductive carbon black using RJH process. (d-e) TEM images of RG with scale bars of 100 nm and 10 nm, respectively. (f) Temperature profile of the whole RJH process. (g) Magnified temperature profile of the graphitization process. (h) Power profile of the whole RJH process.

In this RJH process, the maximum heating power is up to 32 kW (Fig. 1h), significantly less than the 400 kW of the FJH method but much higher than that of general RJH methods (<1 kW).[20,21] Therefore, the Saiyin scale-up Joule heating

system provides a high-power RJH solution for graphitizing conductive carbon sources. The estimated energy consumption for the RJH production of graphene is ~5 kWh kg^{-1} (0.5 \$ kg^{-1}). The entire heating and cooling process takes roughly 10 min, enabling a total of 144 production cycles within 24 h, resulting in the production of over 13.9 kg of graphene, i.e. about 5.0 tons per annual. To the best of our knowledge, producing a nearly 100 g graphene per batch in approximately ten minutes surpasses the capabilities of the other laboratory methods, including flash Joule heating method, chemical vapor deposition, reduction of graphene oxide, and graphite exfoliation (Table S1). Due to its rapid processing, high temperature, and low-cost raw materials, the high-power RJH method presents an efficient and viable approach for the industrial production of graphene, denoted as rapid graphene (RG).

Effect of Joule heating temperature on the structure of RG

To ascertain the optimal conditions to prepare the graphene, carbon black was heated to 2600 °C, 3000 °C, and 3200 °C through RJH methods, denoted as RG-2600, RG-3000, and RG-3200, respectively. The crystalline structure of RGs and carbon black was characterized using X-ray diffraction (XRD) (Fig. 2a). Compared to the broad (002) peak of carbon black, RG-2600, RG-3000 and RG-3200 exhibit a sharp (002) peak and a weak (100) peak and shift to higher angles, indicating complete graphitization of carbon black by the high-power RJH process. The calculated interlayer spacing of RG-2600, RG-3000 and RG-3200 were 0.347, 0.343 and 0.343 nm, respectively (Fig. 2b), larger than that of AB-stacked graphite (0.334 nm). In addition, all (002) peaks of RGs exhibit an asymmetrical shape, featuring a pronounced tail extending towards smaller angles. The characteristics mentioned above suggest that RGs possess a turbostratic structure similar to that reported for flash graphene.[14,17,23]

High-quality graphene can be rapidly identified using Raman spectroscopy. The average Raman spectra of RGs and carbon black were collected from eight sample points (Fig. 2c). The D peak (~1354 cm^{-1}, breathing mode of sp^2-carbon atoms in rings), G peak (~1586 cm^{-1}, bond stretching of all pairs of sp^2-carbon atoms in rings),

and 2D peak (~2703 cm^{-1}, second-order zone boundary phonons in graphene) were observed simultaneously.[24] We assessed the quality of RG by analyzing the defect density using the intensity ratio of D peak to G peak (I_D/I_G), and the graphene conversion ratio using the intensity ratio of 2D peak to G peak (I_{2D}/I_G) (Fig. 2d). Among the three RG samples, RG-3000 exhibited the lowest I_D/I_G, indicating a low defect concentration in the graphene sheets. The smaller error bar of I_{2D}/I_G for RG-3000 also suggested its more uniform graphene structure.[25,26] In addition, the presence of TS_1 (~1861 cm^{-1}) and TS_2 (~1955 cm^{-1}) peaks and the absence of M peak (~1740 cm^{-1}) in RG-2600 and RG-3000 confirmed the turbostratic nature of RG (Fig. S3).[27] While the presence of M peak in RG-3200 demonstrated that a high temperature exceeding 3000 °C can induce the graphene to stack in ordered structure. Consequently, 3000 °C is an optimal temperature for production of turbostratic graphene using the RJH method.

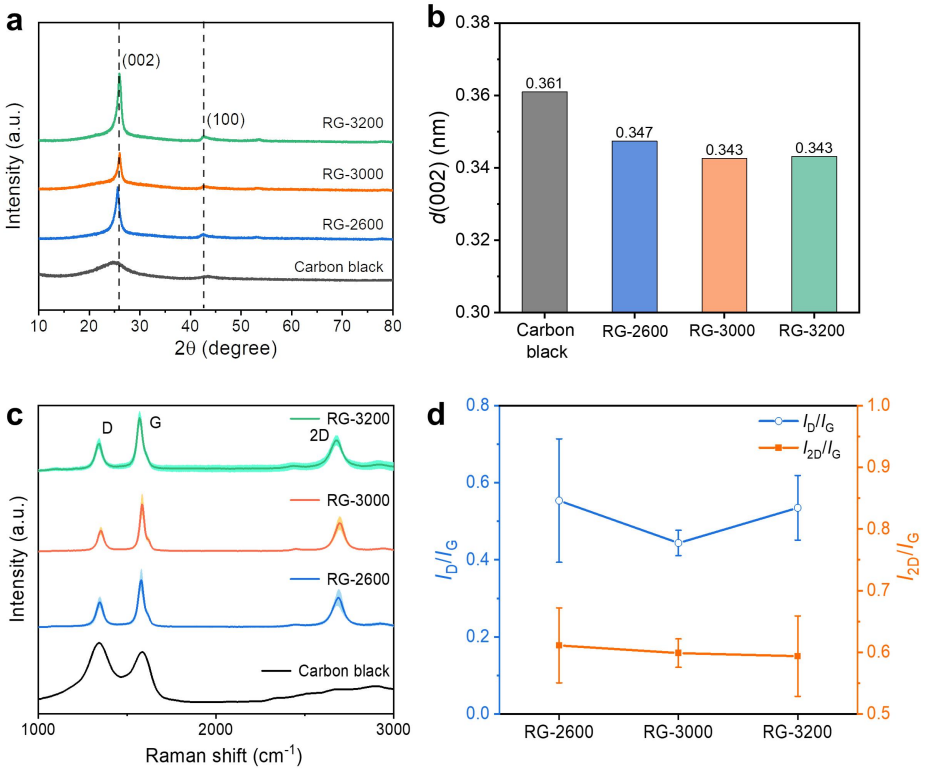

Figure 2. Structural Characterizations of carbon black and RGs produced at different temperatures. (a) XRD patterns, (b) 2θ degree and d(002) interlayer distances, (c) Raman spectra, and (d) I_D/I_G and I_{2D}/I_G ratios.

Mass production of doped graphene

Importantly, this high-power RJH strategy is also applicable for the low-cost and extensive production of doped graphene using various solid dopants. The raw materials of carbon black were mixed with 3 wt% B_2O_3 and 3 wt% melamine, either separately or together, to produce boron-doped RG (B-RG), nitrogen-doped RG (N-RG), and boron-nitrogen-co-doped RG (BN-RG), respectively. X-ray photoelectron spectroscopy (XPS) were employed to determine the chemical states of heteroatoms in doped RG. For B-RG, the atomic content of carbon, oxygen, and boron were 97.08%, 1.61% and 1.31%, respectively, confirming the successful doping of graphene with boron. The bonding types of boron includes B_4C,[28] graphitic B (BC_3),[29] borinic B (C_2BO),[30] and boronic B (CBO_2) species (Fig. S4).[31] For N-RG, only 0.38 wt% of nitrogen atoms was detected (Fig. S5), possibility due to the premature decomposition and volatilization of nitrogen source precursors during the heating process.[32,33] Additionally, dual doping can lead to graphene with high contents of heteroatoms, as it increases the bonding probability and mixing entropy. The atomic contents of carbon, oxygen, nitrogen, and boron in BN-RG were 94.71%, 2.23%, 1.84% and 1.23%, respectively, with the N content significantly higher than that achieved when using only N dopant alone (Fig. S6). The emerging bonding type of B-N indicated the co-doping effect of dual heteroatoms (Fig. S7).

Then we investigated the doping effect on the structural properties of RGs. The doping of boron reduces the interlayer distance of B-RG to 0.341 nm (Fig. S8), possibly due to the electronic deficiency attraction caused by boron defects.[34] The interlayer distance of N-RG and BN-RG was 0.343 nm and 0.344 nm, respectively, which are similar to that of RG. The Raman spectra of B-RG shows a high D peak and a low 2D peak (Fig. 3a), indicating that boron doping introduces more defects into the graphene lattice. As shown in the TEM images (Fig. 3b), B-RG is a polyhedron with more layers. In the Raman spectra of N-RG (Fig. 3c), the mean I_D/I_G intensity ratio is 0.37, even less than that of RG (0.44), indicating that minimal N-doping does not increase the defects in graphene. Notably, the mean I_{2D}/I_G intensity

ration of N-RG is 0.76, significantly higher than that of RG (0.60). This implies that the average number of layers in N-RG is fewer than in RG. TEM images further confirms there are some single-layer graphene sheet in N-RG, as highlighted by yellow circles in Fig. 3d. In addition, the I_{2D}/I_G intensity ratio of BN-NG is between those of B-RG and N-RG (Fig. 3e), and its TEM images show some polyhedron sheets similar to B-RG (Fig. 3f). Therefore, the crystal structure of BN-RG has intermediate characteristics of B-RG and N-RG.

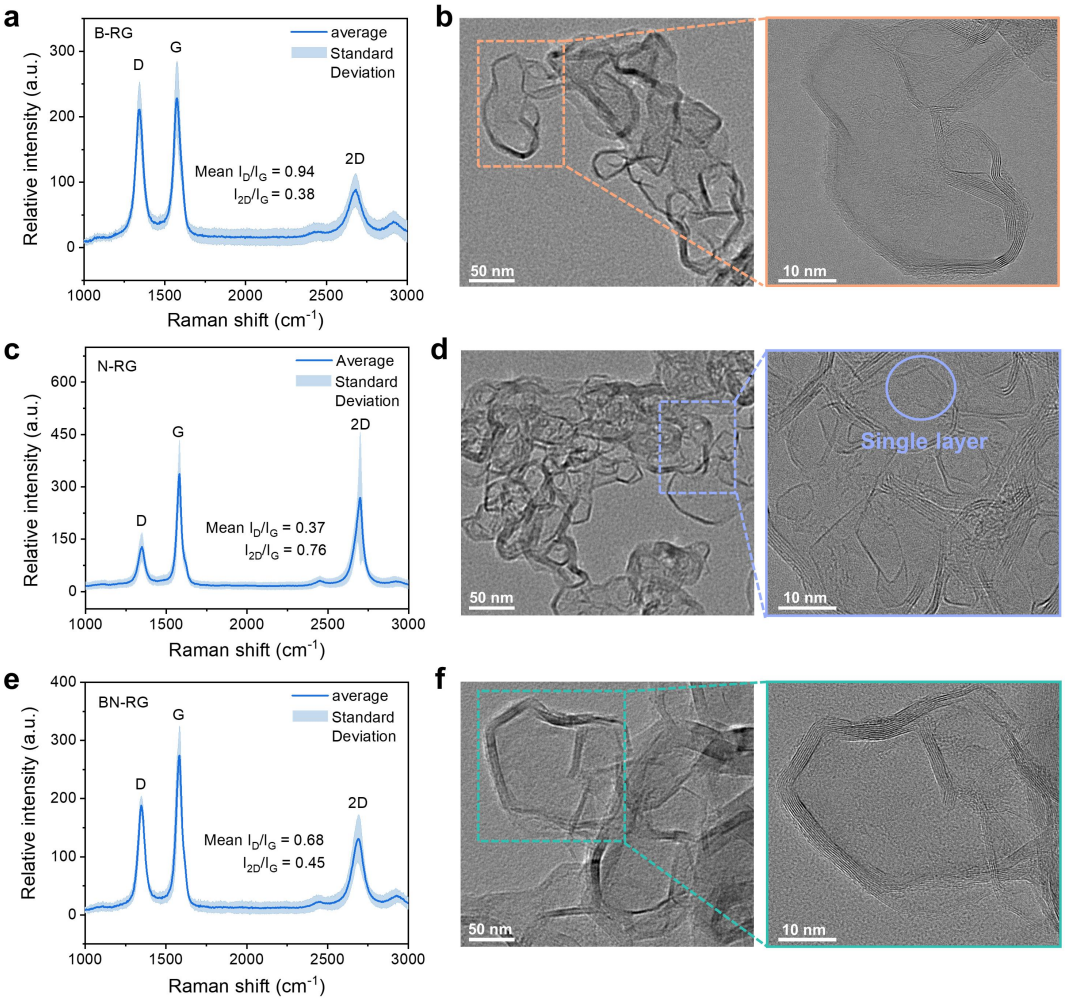

Figure 3. Structural characterizations of B-RG, N-RG, and BN-RG. (a,c,e) Raman spectra, and (b,d,f) TEM images.

Fig. 4a statistically shows the distributions of layers of different RG sheets, as counted from their TEM images (Fig. S9-12). The major thickness of RG, N-RG, and BN-RG are from 3 to 6 layers, while that of B-RG is from 4 to 8 layes. In particularly,

there are plenty of single- and double-layer sheets in N-RG. We believe that the decomposition and gasification of melamine at high temperatures can partly prevent the stacking of layers to produce thinner graphene sheets. In addition, there are about 30% of more than 10 layers in B-RG and BN-RG. Consequently, in the RJH process, the addition of melamine in carbon black can produces thinner graphene sheets, while the addition of boron can produce the thicker sheets.

Physical properties of graphene from RJH method

The primary application of graphene powder is as an additive for reinforcing composite materials and/or enhancing conductivity.[35-37] To achieve optimal bonding with various substrates, the hydrophobicity of the graphene powder should align with the hydrophilicity or hydrophobicity of the substrate material. The contact angle of water is a critical determinant of hydrophilicity or hydrophobicity. The RG powder exhibits hydrophilicity with a contact angle of 74.91°, while contact angles of N-RG, B-RG, and BN-RG decrease to 68.5°, 40.5°, and 51.5° (Fig. 4b), respectively. Heteroatom doping increases the polarity of graphene, thereby enhancing its hydrophilicity and making it suitable as a reinforcing additive in hydrophilic materials.

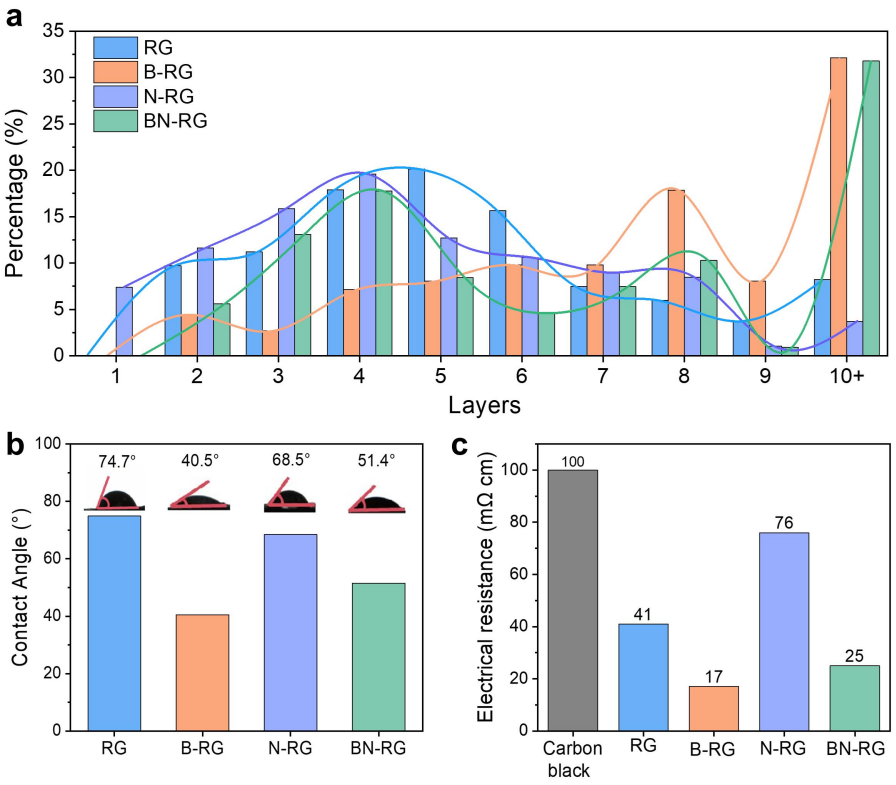

Figure 4. Properties of RG, B-RG, N-RG, and BN-NG. (a) Distribution of layers, (b) contact angles, and (c) powder resistivity of RGs.

The electrical resistivity of RG powder was measured using a powder resistance tester under a pressure of 10 MPa. The graphitization process of RJH converts amorphous carbon in carbon black into RG, resulting in a reduction of resistivity from 100 mΩ·cm to 41 mΩ·cm (Fig. 4c). Among all RGs, B-NG exhibited the lowest resistivity of 17 mΩ·cm, which may be attributed to the boron doping lowering the graphitization temperature and enhancing the structural integrity of the graphene sheets.[34] On the contrary, nitrogen doping reduces the conductivity of graphene due to the smaller sizes of N-RG sheets, which increase contact resistance.

Conclusion

In this work, we developed a high-power RJH method for massively and high yields producing graphene. The high-power RJH process uses a scale-up Joule heating system with compressing 100 g of carbon black in a quartz tube, achieving temperatures up to 3000°C in 250 s. The transformation process of graphene consists of carbonization and graphitization phases, with extremely low energy consumption

of ~5 kWh kg^{-1} (0.5 $ kg^{-1}). Theoretically, one device has the potential to generate as much as 5 tons of graphene annually. Additives like melamine and boron oxide are used for direct production of doped graphene. N-RG showed reduced sheet layers, while B-RG and BN-RG exhibited thicker sheets and increased conductivity. Consequently, these additives hold significant appeal for modifying the local structure and quality of RGs. Considering the extraordinary advantages encompassing exceptional great energy and time efficiency, decent product homogeneity, and structural modifiability, we anticipate that this high-power RJH method will show unlimited potentials in mass graphene production for industrial applications.

EXPERIMENTAL SECTION

Materials

Conductive carbon black (Type: HCD-5) was purchased from Tianjin Huacai Co., LTD. Melamine (≥99.5%) was purchased from Tianjin Kemio Chemical Reagent Co., LTD. Boric oxide (≥99%) was purchased from Shanghai Hongri Chemical Co., LTD.

Preparation of granulated carbon black

To load more samples in the quartz tube, conductive carbon black, water, and any required additives were uniformly mixed and processed into granules with diameters of 3 mm using a double-roller granulator, followed by drying.

RJH System

The high-power rapid Joule heating processes were performed using the SaiYin scale-up Joule heating system from Saiyin Materials Co., LTD. The quartz tube used for the 100 g sample had an inner diameter of 55 mm, an outer diameter of 65 mm, and a length of 200 mm. Two graphite electrodes with a diameter of 54 mm were used to connect and compress the sample grains. Two graphite electrodes with a diameter of 54 mm were used to connect and compress the sample grains.

Characterizations

Raman spectra from eight randomly selected points on each sample were obtained using a Horiba Jobin-Yvon LabRAM ARAMIS system with a 532 nm wavelength laser. XRD patterns of RG, B-RG, N-RG, and BN-RG were collected on a Rigaku D/Max-RB, with a 2θ range between 10° and 80°, at room temperature. TEM images were collected using a JEM-2100F instrument operated at 200 kV. All samples were sonicated for 15 minutes and dispersed in an ethanol solution prior to testing. XPS data were collected using a Thermo Scientific K-Alpha instrument. Contact angle measurements were conducted using a JY-82C instrument. Due to the sample's good water absorption and rapid droplet uptake, video recording was employed to capture

images every 62 ms. The image of the droplet just in contact with the sample was used to measure the contact angle. Powder resistivity data were obtained using a semiconductor powder resistivity tester (DC-4). The powder sample was evenly distributed in the sample tank, and the resistivity value was recorded at a pressure of 10 MPa.

Supporting Information

The Supporting Information is available free of charge at https://xxx.xxx.xxx.

Equipment, TEM, and other images; XPS and Raman spectra; additional graphs (PDF)

Conflict interest

The authors declare there is no competing financial interest(s).

Acknowledgments

The authors thank Quanfu Zhang and Chaochao Guo of Saiyin Materials Co., LTD. for providing scale-up Joule heating system for the experiments. This work was supported by NSFC 21473106.

References

1. Geim, A. K., Novoselov, K. S. The rise of graphene. *Nat. Mater.* **6**, 183-191 (2007).
2. Novoselov, K. S. *et al.* Electric field effect in atomically thin carbon films. *Science* **306**, 666-669 (2004).
3. Bolotin, K. I. *et al.* Ultrahigh electron mobility in suspended graphene. *Solid State Commun.* **146**, 351-355 (2008).
4. Papageorgiou, D. G., Kinloch, I. A., Young, R. J. Mechanical properties of graphene and graphene-based nanocomposites. *Prog. Mater. Sci.* **90**, 75-127 (2017).
5. Peng, Z. *et al.* Flexible boron-doped laser-induced graphene microsupercapacitors. *ACS Nano* **9**, 5868-5875 (2015).

6. Agnoli, S., Favaro, M. Doping graphene with boron: a review of synthesis methods, physicochemical characterization, and emerging applications. *J. Mater.* **4**, 5002-5025 (2016).

7. Barkan T. *et al.* Mapping the landscape for graphene commercialization., Nat. Rev. Phys., (2024) DOI:10.1038/s42254-024-00754-9.

8. Lin, L., Peng, H., Liu, Z. Synthesis challenges for graphene industry. *Nat. Mater.* **18**, 520-524 (2019).

9 . Li, X. *et al.* Large-area synthesis of high-quality and uniform graphene films on copper foils. *Science* **324**, 1312-1314 (2009).

10. Marcano, D. C. *et al.* Improved synthesis of graphene oxide. *ACS Nano* **4**, 4806-4814 (2010).

11. Xu, Y., Cao, H., Xue, Y., Li, B., Cai, W. Liquid-phase exfoliation of graphene: an overview on exfoliation media, techniques, and challenges. *Nanomaterials* **8**, 942 (2018).

12. Islam, A., Mukherjee, B., Pandey, K. K., Keshri, A. K. Ultra-fast, chemical-free, mass production of high quality exfoliated graphene. *ACS Nano* **15**, 1775-1784 (2021).

13. Paton, K. R. *et al.* Scalable production of large quantities of defect-free few-layer graphene by shear exfoliation in liquids. *Nat. Mater.* **13**, 624-630 (2014).

14. Luong, D. X. *et al.* Gram-scale bottom-up flash graphene synthesis. *Nature* **577**, 647-651 (2020).

15. Zhu, X. *et al.* Continuous and low-carbon production of biomass flash graphene. *Nat. Commun.* **15**, 3218 (2024).

16. Eddy, L. *et al.* Electric Field Effects in Flash Joule Heating Synthesis. *J. Am. Chem. Soc.* **146**, 16010-16019 (2024).

17. Stanford, M. G., *et al.* Flash graphene morphologies. *ACS Nano* **14**, 13691-13699 (2020).

18. Eddy, L. *et al.* Automated Laboratory Kilogram-Scale Graphene Production from Coal. *Small Methods* **8**, 2301144 (2024).

19. Yao, Y. *et al.* Carbon welding by ultrafast joule heating. *Nano Lett.* **16**, 7282-7289 (2016).
20. Yao, Y. *et al.* Carbothermal shock synthesis of high-entropy-alloy nanoparticles. *Science* **359**, 1489-1494 (2018).
21. Wang, C. *et al.* A general method to synthesize and sinter bulk ceramics in seconds. *Science* **368**, 521-526 (2020).
22. Franklin, R. E. Crystallite growth in graphitizing and non-graphitizing carbons. *Proc. R. Soc. Lond* **209**, 196-218 (1951).
23. Li, Z., Lu, C., Xia, Z., Zhou, Y., Luo, Z. X-ray diffraction patterns of graphite and turbostratic carbon. *Carbon* **45**, 1686-1695 (2007).
24. Malard, L. M., Pimenta, M. A., Dresselhaus, G., Dresselhaus, M. S. Raman spectroscopy in graphene. *Phys. Rep.* **473**, 51-87 (2009).
25. Pollard, A. J. *et al.* Quantitative characterization of defect size in graphene using Raman spectroscopy. *Appl. Phys. Lett.* **105**, (2014).
26. Jorio, A., Ferreira, E. H. M., Moutinho, M. V., Stavale, F., Achete, C. A., Capaz, B. Measuring disorder in graphene with the G and D bands. *Phys. Status Solidi* **247**, 2980-2982 (2010).
27. Garlow, J. A., Barrett, L. K., Wu, L., Kisslinger, K., Zhu, Y., Pulecio, J. F. Large-area growth of turbostratic graphene on Ni (111) via physical vapor deposition. *Sci. Rep.* **6**, 19804 (2016).
28. Cermignani, W., Paulson, T. E., Onneby, C., Pantano, C. G. Synthesis and characterization of boron-doped carbons. *Carbon* **33**, 367-374 (1995).
29. Shirasaki, T., Derré, A., Ménétrier, M., Tressaud, A., Flandrois, S. Synthesis and characterization of boron-substituted carbons. *Carbon* **38**, 1461-1467 (2000).
30. Jacques, S., Guette, A., Bourrat, X., Langlais, F., Guimon, C., Labrugère, C. LPCVD and characterization of boron-containing pyrocarbon materials. *Carbon* **34**, 1135-1143 (1996).
31. Van Khai, T. *et al.* Comparison study of structural and optical properties of boron-doped and undoped graphene oxide films. *Chem. Eng. J.* **211**, 369-377

(2012).

32. Chen, W. *et al.* Heteroatom-doped flash graphene. *ACS Nano* **16**, 6646-6656 (2022).

33. Zhu, S. *et al.* Flash nitrogen-doped graphene for high-rate supercapacitors. *ACS Mater. Lett.* **4**, 1863-1871 (2022).

34. Ōya, A., Yamashita, R., Ōtani, S. Catalytic graphitization of carbons by borons. *Fuel* **58**, 495-500 (1979).

35. Advincula, P. A. *et al.* Ultra-High Loading of Coal-Derived Flash Graphene Additives in Epoxy Composites. *Macromol. Mater. Eng.* **308**, 2200640 (2023).

36. Advincula, P. A. *et al.* Waste plastic-and coke-derived flash graphene as lubricant additives. *Carbon* **203**, 876-885 (2023).

37. Damasceno, B. S. *et al.* Flash graphene and poly (o-methoxy aniline) for the composition of a solvent-based conductive ink. *Surf.* **50**, 104427 (2024).